Basal Brain Oxidative and Nitrative Stress Levels Are Finely Regulated by the Interplay Between Superoxide Dismutase 2 and p53

Article *in* Journal of Neuroscience Research · August 2015

DOI: 10.1002/jnr.23627

8 authors, including:

Eugenio Barone
Sapienza University of Rome
60 PUBLICATIONS **1,274** CITATIONS
SEE PROFILE

Fabio Di Domenico
Sapienza University of Rome
90 PUBLICATIONS **1,544** CITATIONS
SEE PROFILE

Marzia Perluigi
Sapienza University of Rome
115 PUBLICATIONS **3,595** CITATIONS
SEE PROFILE

D. Allan Butterfield
University of Kentucky
638 PUBLICATIONS **40,455** CITATIONS
SEE PROFILE

Journal of Neuroscience Research 00:00–00 (2015)

Basal Brain Oxidative and Nitrative Stress Levels Are Finely Regulated by the Interplay Between Superoxide Dismutase 2 and p53

Eugenio Barone,[1,2] Giovanna Cenini,[3,4,5] Fabio Di Domenico,[1] Teresa Noel,[5,6] Chi Wang,[7] Marzia Perluigi,[1] Daret K. St. Clair,[5,6] and D. Allan Butterfield[3,4,5]*

[1]Department of Biochemical Sciences "A. Rossi-Fanelli," Sapienza University of Rome, Roma, Italy
[2]Facultad de Salud, Instituto de Ciencias Biomédicas, Universidad Autónoma de Chile, Providencia, Santiago, Chile
[3]Department of Chemistry, University of Kentucky, Lexington, Kentucky
[4]Sanders-Brown Center on Aging, University of Kentucky, Lexington, Kentucky
[5]Markey Cancer Center, University of Kentucky, Lexington, Kentucky
[6]Department of Toxicology, University of Kentucky, Lexington, Kentucky
[7]Biostatistics Core, Markey Cancer Center, University of Kentucky, Lexington, Kentucky

Superoxide dismutases (SODs) are the primary reactive oxygen species (ROS)-scavenging enzymes of the cell and catalyze the dismutation of superoxide radicals O_2^- to H_2O_2 and molecular oxygen (O_2). Among the three forms of SOD identified, manganese-containing SOD (MnSOD, SOD2) is a homotetramer located wholly in the mitochondrial matrix. Because of the SOD2 strategic location, it represents the first mechanism of defense against the augmentation of ROS/reactive nitrogen species levels in the mitochondria for preventing further damage. This study seeks to understand the effects that the partial lack ($SOD2^{-/+}$) or the overexpression (TgSOD2) of MnSOD produces on oxidative/nitrative stress basal levels in different brain isolated cellular fractions (i.e., mitochondrial, nuclear, cytosolic) as well as in the whole-brain homogenate. Furthermore, because of the known interaction between SOD2 and p53 protein, this study seeks to clarify the impact that the double mutation has on oxidative/nitrative stress levels in the brain of mice carrying the double mutation ($p53^{-/-} \times SOD2^{-/+}$ and $p53^{-/-} \times$ TgSOD2). We show that each mutation affects mitochondrial, nuclear, and cytosolic oxidative/nitrative stress basal levels differently, but, overall, no change or reduction of oxidative/nitrative stress levels was found in the whole-brain homogenate. The analysis of well-known antioxidant systems such as thioredoxin-1 and Nrf2/HO-1/BVR-A suggests their potential role in the maintenance of the cellular redox homeostasis in the presence of changes of SOD2 and/or p53 protein levels.

Key words: oxidative stress; MnSOD; p53; biliverdin reductase-A; heme oxygenase-1; RRID:AB_10850321; RRID:AB_1840351; RRID:AB_2256876; RRID:AB_10618757; RRID:AB_2049199; RRID:AB_881705; RRID:AB_476744; RRID:AB_958795

Mitochondria are the major source of reactive oxygen species (ROS) under normal physiological conditions, superoxide radicals (O_2^-) being the primary ROS produced by this organelle (Holmstrom and Finkel, 2014). Reactive nitrogen species (RNS; nitric oxide synthase [NOS]-produced NO and molecules derived from NO, such as peroxynitrite and NO_2) represent the other reactive species widely studied for their role in cellular redox homeostasis (Poon et al., 2004; Calabrese et al., 2007; Holmstrom and Finkel, 2014).

Independently of the locus where they are generated, ROS and RNS are able to spread into the intracellular space, where they play an important role in the activation or inhibition of specific redox signaling-regulated events (e.g., cell proliferation, cell death, gene

SIGNIFICANCE:

This is the first study highlighting changes that occur with regard to basal oxidative and nitrative stress levels in mice brain following MnSOD partial lack ($SOD2^{-/+}$) or overexpression (TgSOD2). We provide data on how changes occurring in different cellular compartments (mitochondria, nucleus, cytosol) finally impact the status of the whole cell. Furthermore, this study provides new insights into the interconnectivity of MnSOD, p53, and oxidative stress in the brain.

Contract grant sponsor: NIH (to D.A.B., D.K.S.C.).

*Correspondence to: Prof. D. Allan Butterfield, Department of Chemistry, Markey Cancer Center, and Sanders-Brown Center on Aging, University of Kentucky, Lexington, KY 40506-0055. E-mail: dabcns@uky.edu

Received 29 April 2015; Revised 23 July 2015; Accepted 23 July 2015

Published online 00 Month 2015 in Wiley Online Library (wileyonlinelibrary.com). DOI: 10.1002/jnr.23627

expression) by directly or indirectly promoting the reversible oxidation/reduction, phosphorylation/dephosphorylation, and nitrosylation/denitrosylation of specific amino acids (Hancock et al., 2001; Calabrese et al., 2007; Holley et al., 2011; Holmstrom and Finkel, 2014). Conversely, if the amount of ROS and RNS exceeds the capacity of the antioxidant defense systems, an imbalanced oxidative system causes damage to cell components (Perluigi et al., 2012; Cobb and Cole, 2015).

Superoxide dismutases (SODs) are the primary ROS-scavenging enzymes of the cell, and they catalyze the dismutation of superoxide radicals O_2^- to H_2O_2 and molecular oxygen (O_2; Holley et al., 2011; Pani and Galeotti, 2011). The three forms of SOD, encoded by different genes, are 1) copper- and zinc-containing SOD (SOD1), 2) extracellular SOD (SOD3), and 3) manganese-containing SOD (MnSOD; SOD2; Holley et al., 2011; Pani and Galeotti, 2011). Because of its strategic localization in the mitochondrial matrix, SOD2 is thought to be a first-line defense for protecting mitochondria against oxidative/nitrative damage (Zorov et al., 2006; Holley et al., 2011), which otherwise would lead to a vicious cycle in which mitochondrial ROS/RNS causes oxidative damage to mitochondrial DNA, leading to further mitochondrial dysfunction and oxidant generation (Miriyala et al., 2011). In line with this, SOD2 has been demonstrated to be the only form of SOD absolutely essential for life (Gregory and Fridovich, 1973; Li et al., 1995; Duttaroy et al., 2003; Holley et al., 2010).

Because of these essential features of SOD2, its role in the brain is of great interest, especially in the context of neuronal energy metabolism. Indeed, neurons rely on an elevated oxidative metabolism (which occurs in the mitochondria) to meet their high energy requirements, with a consequent physiological production of both ROS and RNS (Belanger et al., 2011). Although on the one hand controlled ROS and RNS production is required for the maintenance of synaptic plasticity, long-term potentiation, and neuronal plasticity (Calabrese et al., 2007; Chatoo et al., 2011; Holmstrom and Finkel, 2014), on the other hand the brain is rich in polyunsaturated fatty acid and iron, two features that, coupled with high oxygen usage and a low antioxidant capacity, make the brain particularly susceptible to oxidative damage (Belanger et al., 2011). In this picture, variations of SOD2 activity could affect ROS/RNS levels either positively or negatively, thus driving, at least in part, the fate of the mitochondria and, probably, of the entire neuron. Indeed, alterations of SOD2 activity can result in numerous pathological phenotypes in the brain, such as Alzheimer's disease, Parkinson's disease, stroke, or simply aging (Flynn and Melov, 2013). Thus, although the regulation of oxidative stress alone does not seem to prevent specific neurodegenerative disorders, it may provide some benefit in slowing the progression of these diseases and help to maintain the bioenergetic function of neurons (Flynn and Melov, 2013).

Although previous articles describing studies performed with heterozygous SOD2 knockout mice and with transgenic mice have reported on the effects associated with the reduction (Li et al., 1995; Van Remmen et al., 2003; Jang and Van Remmen, 2009; Holley et al., 2010) or the overexpression (Jang and Van Remmen, 2009; Jang et al., 2009) of SOD2 in different tissues, no published studies have evaluated the impact in the brain under basal conditions.

This work seeks to evaluate the effects that the partial lack ($SOD2^{-/+}$) or the overexpression (TgSOD2) of SOD2 produce on the basal levels of oxidative and nitrative stress in mouse brain. Furthermore, because of the known interaction between SOD2 and p53 protein (Zhao et al., 2005; Holley et al., 2010; Miriyala et al., 2011; Pani and Galeotti, 2011) and from previous studies by our group demonstrating for the first time that the lack of p53 significantly reduces basal protein oxidation and lipid peroxidation in the brain of $p53^{-/-}$ mice at least in part through the upregulation of SOD2 (Barone et al., 2012; Fiorini et al., 2012), this study seeks to clarify the impact that the double mutation has on oxidative/nitrative stress levels in the brain of $p53^{-/-} \times SOD2^{-/+}$ and $p53^{-/-} \times$ TgSOD2 mice. We performed studies to test the hypothesis that changes with regard to oxidative/nitrative stress levels are linked to the regulation of an integrated network of mechanisms that are under the control of genes strictly involved in preserving cellular homeostasis during stressful conditions, named "vitagenes," such as those encoding for thioredoxin-1, members of the heme-oxygenase-1/biliverdin reductase-A (HO-1/BVR-A) system, and nuclear factor erythroid 2-related factor 2 (Nrf-2).

MATERIALS AND METHODS

Chemicals

All chemicals were purchased from Sigma-Aldrich (St. Louis, MO) unless otherwise stated. Nitrocellulose membranes were obtained from Bio-Rad (Hercules, CA). Anti-rabbit IgG horseradish peroxidase conjugate secondary antibody was obtained from GE Healthcare (Piscataway, NJ).

Animals

Heterozygous mice $p53^{-/+}$, $p53^{-/+} \times SOD2^{+/-}$, and $p53^{-/+} \times$ TgSOD2 overexpressors were gifts from Dr. Holly Van Remmen, then at the University of Texas San Antonio Health Sciences Center. $p53^{-/+}$ Mice were crossed with $p53^{-/+} \times SOD2^{-/+}$- and $p53^{-/+} \times$ TgSOD2-overexpressing mice to create $p53^{-/-}$ knockout mice and wild-type (WT) littermates. Crosses of $p53^{-/-}$ with $SOD2^{+/-}$ heterozygous knockdown and of $p53^{-/-}$ knockout mice with TgSOD2-overexpressing mice were used to create $p53^{-/-} \times SOD2^{+/-}$- and $p53^{-/-} \times$ TgSOD2-overexpessing mice, respectively, which were used in the present studies. Dr. Tyler Jacks of the Center for Cancer Research and Department of Biology, Massachusetts Institute of Technology, initially generated the $p53^{-/-}$ mice on a C56BL/6 background. Male mice between 10 and 12 weeks old were used in all studies. All animal experimental procedures were approved by the Institutional Animal Care and Use Committee of the University of Kentucky and followed the NIH *Guidelines for the care and use of laboratory animals*.

Cellular Fractions, Isolation, and Purification

Mice were humanely euthanized, and the brain was promptly removed. Cellular fractions were immediately isolated from the freshly obtained brain by using Percoll gradients (Sims, 1990), with minor modifications. Whole brain was suspended in ice-cold isolation buffer (250 mM sucrose, 10 mM HEPES, and 1 mM potassium EDTA, pH 7.2) and homogenized by six passes with a motor-driven Teflon pestle. The homogenate was then centrifuged at 1,330*g* for 3 min at 4°C. The supernatant was carefully decanted and saved, and the resulting pellet was resuspended in isolation buffer and once more centrifuged at 1,330*g* for 3 min. The resulting pellet (nuclear fraction) was saved, and the supernatants from both spins were combined and spun at 21,200*g* for 10 min at 4°C. The supernatant (cytosolic fraction) was saved, and the resulting pellet (containing mitochondria) was resuspended in 15% Percoll solution (v/v in isolation buffer) and layered onto discontinuous Percoll gradients of 23% and 40% Percoll (v/v in isolation buffer). Gradients were spun at 30,700*g* for 5 min at 4°C. At the 23–40% Percoll interface, mitochondria were isolated and resuspended in respiration buffer (250 mM sucrose, 2 mM magnesium chloride, 20 mM HEPES, and 2.5 mM phosphate buffer, pH 7.2) and centrifuged at 16,700*g* for 10 min at 4°C. The pellet was resuspended in respiration buffer and centrifuged at 6,900*g* for 10 min at 4°C, and the resulting pellet was washed in phosphate-buffered saline (PBS) at 6,900*g* for 10 min at 4°C. The pellet was finally resuspended in 0.5–1.0 ml PBS. Protein concentration was determined by the Pierce BCA method (Pierce, Rockford, IL).

Slot-Blot Analysis

Total protein carbonyl (PC) levels. Samples (5 μl) of each fraction as well as of whole homogenate, 12% sodium dodecyl sulfate (SDS; 5 μl), and 10 μl of 10× diluted 2,4-dinitrophenylhydrazine (DNP) from 200 mM stock were incubated at room temperature for 20 min, followed by neutralization with 7.5 μl neutralization solution (2 M Tris in 30% glycerol). Protein (250 ng) was loaded into each well on a nitrocellulose membrane under vacuum with a slot-blot apparatus. The membrane was blocked in blocking buffer (3% bovine serum albumin [BSA]) in PBS 0.01% (w/v) sodium azide and 0.2% (v/v) Tween 20 (PBST) for 1 hr and incubated with an anti-DNP adducts polyclonal antibody (1:100; catalog No. MAB2223; RRID:AB_10850321; EMD Millipore, Billerica, BA) in PBST for 1 hr. After primary antibody incubation, the membrane was washed in PBS three times for 5 min each. After having been washed, the membrane was incubated with an anti-rabbit IgG alkaline phosphatase secondary antibody diluted in PBS at 1:8,000 for 1 hr. The membrane was washed in PBS three times for 5 min each and developed with Sigma Fast tablets (5-bromo-4-chloro-3-indolyl phosphate/nitroblue tetrazolium [BCIP/NBT] substrate). Blots were dried, scanned with Adobe Photoshop CS2 (RRID:SciRes_000161; Adobe Systems, San Jose, CA), and quantified in Scion Image (RRID:nif-0000–33408, PC version of Macintosh-compatible NIH Image). No nonspecific binding of antibody to the membrane was observed.

Total protein-bound 4-hydroxy-2-nonenals (HNE) and 3-nitrotyrosine (3-NT) levels. Samples (5 μl) of each fraction as well as of whole homogenate, 12% SDS (5 μl), 5 μl modified Laemmli buffer containing 0.125 M Tris base, pH 6.8, 4% (v/v) SDS, and 20% (v/v) glycerol were incubated for 20 min at room temperature and were loaded (250 ng) into each well on a nitrocellulose membrane in a slot-blot apparatus under vacuum. The membrane was treated as described above and incubated with an antiprotein- bound HNE polyclonal antibody (1:2,000; catalog No. NB100–63093; RRID:AB_958795) or an anti-3-NT antibody (1:2,000; catalog No. N5538; RRID:AB_1840351) in PBS for 90 min. The membranes were further developed and quantified as described above. A faint background staining resulting from the antibody alone was observed, but because each sample had a control this minor effect was controlled.

Western Blot Analysis

For Western blot analyses, protein levels were analyzed based on their cellular localization in the whole cell, HO-1 and thioredoxin-1 in membrane fractions, and BVR-A and Nrf-2 in both cytosolic and nuclear fractions. Briefly, 50 μg protein was denaturated in sample buffer for 5 min at 100°C, and proteins were separated on 12% precast Criterion gels (Bio-Rad) by electrophoresis at 100 mA for 2 hr in 3-(N-morpholino)propanesulfonic acid buffer (Bio-Rad) into the Bio-Rad apparatus. The proteins from the gels were then transferred to nitrocellulose membrane with the Transblot-Blot SD semidry transfer cell (Bio-Rad) at 20 mA for 2 hr. Subsequently, the membranes were blocked for 1 hr at 4°C with fresh blocking buffer consisting of 3% BSA in PBST. The membranes were incubated at room temperature in PBST for 2 hr with the following primary antibodies, as separate experiments: polyclonal anti-rabbit thioredoxin 1 (1:1,000; catalog No. sc-20146; RRID:AB_2256876; Santa Cruz Biotechnology, Santa Cruz, CA), polyclonal anti-rabbit HO-1 (1:1,000; catalog No. ADI-SPA-895; RRID:AB_10618757; Enzo Life Sciences, Farmingdale, NY), polyclonal anti-rabbit BVR-A (1:5,000; catalog No. ab90491; RRID:AB_2049199; Abcam, Cambridge, MA), polyclonal anti-rabbit Nrf-2 (1:1,000; catalog No. ab31163; RRID:AB_881705; Abcam), and polyclonal anti-rabbit β-actin (1:2,000; catalog No. A5441; RRID:AB_476744). The membranes were then washed three times for 5 min each with PBST, followed by incubation with an alkaline phosphatase- or horseradish peroxidase-conjugated secondary antibody (1:5,000) in PBST for 2 hr at room temperature. Membranes were then washed three times in PBST for 5 min each and developed with BCIP/NBT color developing reagent for alkaline phosphatase secondary antibody or ECL plus Western blotting detection reagents for horseradish peroxidase-conjugated secondary antibody. Blots were dried, scanned in TIF format with Adobe Photoshop on a Canoscan 8800F (Canon, Tokyo, Japan) or Storm UV transilluminator ($\lambda ex = 470$ nm, $\lambda em = 618$ nm; Molecular Dynamics, Sunnyvale, CA) for chemiluminescence. The images were quantified in Image Quant TL 1D v.7.0 (GE Healthcare). The optical density of bands was calculated as volume (optical density × area) adjusted for the background.

TABLE I. Primary Antibodies Used

Antigen	Description of immunogen	Source, host species, catalog No., clone or lot No., RRID	Concentration used
DNP adducts	KLH-conjugated DNP	EMD Millipore, mouse, MAB2223, clone 9H8.1, RRID:AB_10850321	1:100 (Slot-blot assay)
HNE	HNE conjugate	Novus Biologicals (Littleton, CO), goat, NB100–63093, RRID:AB_958795	1:2,000 (Slot-blot assay)
3-NT	3-NT-KLH	Sigma-Aldrich, mouse, N5538, clone 18G4, RRID:AB_1840351	1:2,000 (Slot-blot assay)
Thioredoxin-1	Amino acids 1–105 representing full-length thioredoxin of human origin	Santa Cruz Biotechnology, rabbit, sc-20146, RRID:AB_2256876	1:1,000 (WB)
HO-1	Recombinant rat HO-1 (Hsp32) lacking the membrane-spanning region	Enzo Life Sciences, rabbit, ADI-SPA-895, RRID:AB_10618757	1:1,000 (WB)
BVR-A	Recombinant rat biliverdin reductase expressed in *Escherichia coli*	Abcam, rabbit, ab90491, RRID:AB_2049199	1:5,000 (WB)
Nrf-2	Synthetic peptide: TL YLEVFSMLRD EDGKPYSP, corresponding to amino acids 569–588 of human Nrf-2	Abcam, rabbit, ab31163, RRID:AB_881705	1:1,000 (WB)
ß-Actin	Synthetic β-actin cytoplasmic N-terminal peptide Ac-Asp-Asp-Asp-Ile-Ala-Ala-Leu-Val-Ile-Asp-Asn-Gly-Ser-Gly-Lys conjugated to KLH	Sigma-Aldrich, mouse, A5441, clone AC-15, RRID:AB_476744	1:2,000 (WB)

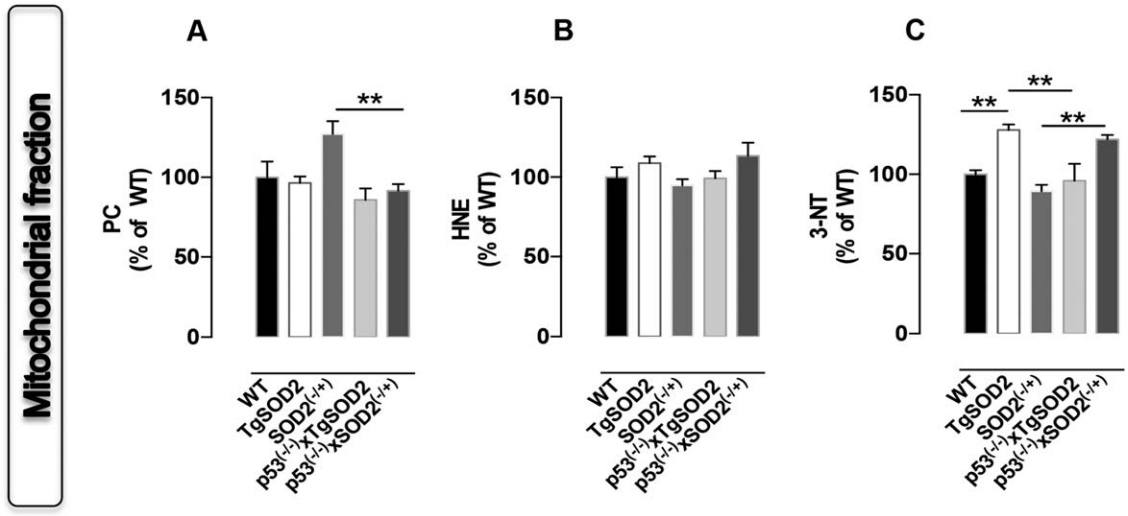

Fig. 1. In vivo oxidative and nitrative modifications observed in mitochondria isolated from the brains of WT, SOD2 transgenic (TgSOD2), and SOD2 heterozygous knockout ($SOD2^{-/+}$) mice and of mice carrying the double mutation ($p53^{-/-}$ × TgSOD2, $p53^{-/-}$ × $SOD2^{-/+}$). PC (**A**), protein-bound HNE (**B**), and 3-NT (**C**) levels measured in the mitochondrial fraction. Densitometric values are percentage of the WT group, set as 100%. Data are mean ± SE of three replicates of each individual sample (n = 6) per group. $^{**}P < 0.01$ vs. WT or the corresponding single-mutant mice (ANOVA).

Antibody Characterization

See Table I for a list of all antibodies used. With regard to slot-blot analyses for the evaluation of total PC, HNE, and 3-NT levels in our samples, each of the antibodies used (anti-DNP, anti-HNE, and anti-3-NT) recognizes specific oxidative modifications (see Table I) to protein structure, resulting in higher or lower colored spots depending on the levels of the modification assayed (Sultana and Butterfield, 2008). For Western blot of mouse brain isolated fractions, the antithioredoxin-1 antibody recognizes a single band of ~12 kDa, the anti-HO-1 antibody recognizes a single band of ~32 kDa, the anti-BVR-A antibody recognizes a single band of ~33 kDa, the anti-Nrf-2 antibody recognizes a single band of ~68 kDa, and the anti-β-actin antibody recognizes a single band of ~42 kDa.

Statistical Analysis

Data are expressed as mean ± SE of six independent samples per group. All statistical analyses were performed in

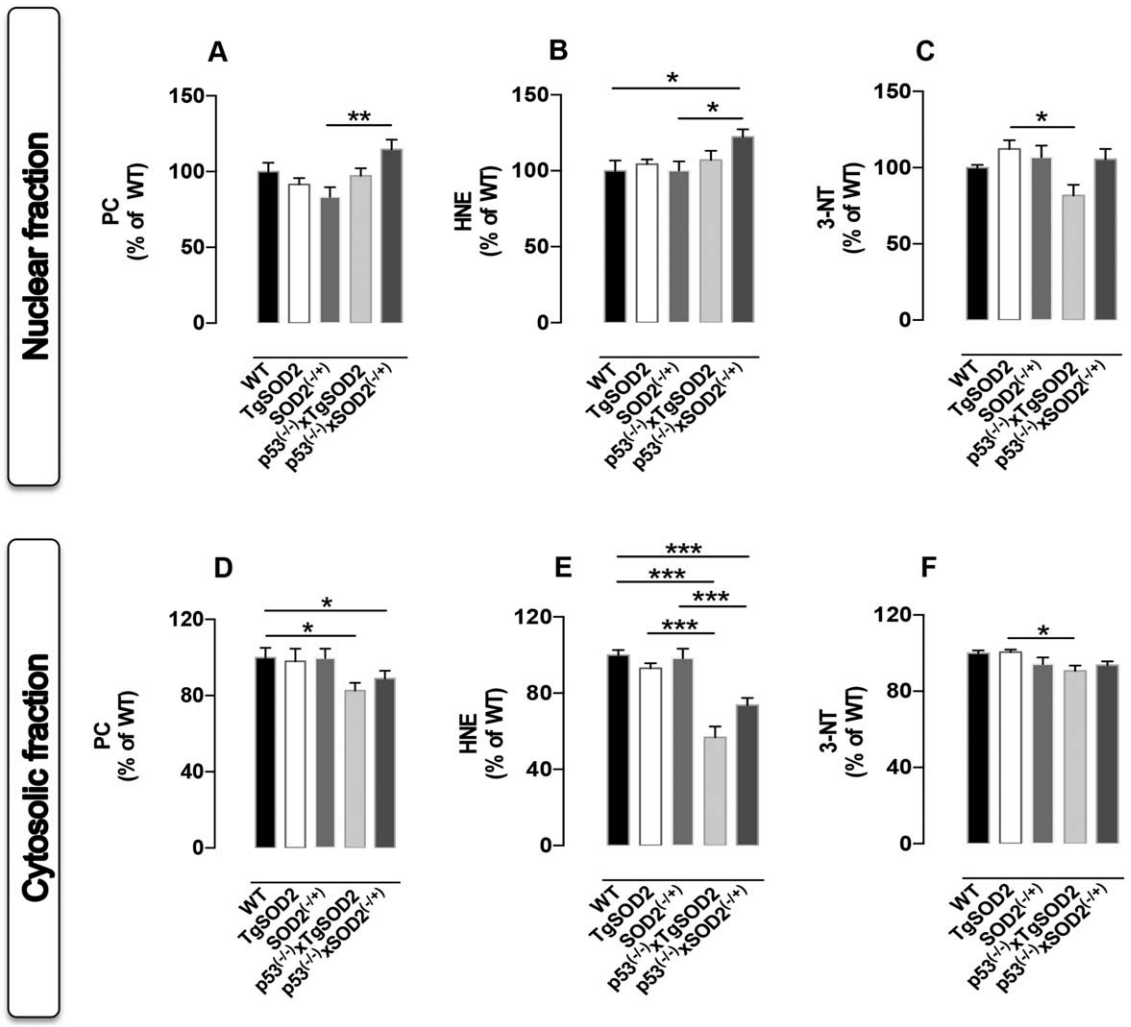

Fig. 2. In vivo oxidative and nitrative modifications observed in nuclei and cytosol isolated from the brains of WT, SOD2 transgenic (TgSOD2), and SOD2 heterozygous knockout ($SOD2^{-/+}$) mice and of mice carrying the double mutation ($p53^{-/-} \times$ TgSOD2, $p53^{-/-} \times SOD2^{-/+}$). PC (**A**), protein-bound HNE (**B**), and 3-NT (**C**) levels measured in the nuclear fraction. PC (**D**), HNE (**E**), and 3-NT (**F**) levels measured in the cytosolic fraction. Densitometric values are percentage of the WT group, set as 100%. Data are mean ± SE of three replicates of each individual sample (n = 6) per group. $\star P < 0.05$, $\star\star P < 0.01$, and $\star\star\star P < 0.001$ vs. WT or the corresponding single-mutant mice (ANOVA).

GraphPad Prism (RRID:nlx_156835; GraphPad Software, La Jolla, CA) by nonparametric one-way ANOVA with post hoc Tukey *t*-test. $P < 0.05$ was considered significantly different.

RESULTS

Basal Oxidative and Nitrative Stress Levels Evaluated in Brain Isolated Mitochondria

To clarify the contribution of SOD2 to basal brain oxidative and nitrative stress, PC, protein-bound HNE, and 3-NT levels were first assayed in the mitochondrial fraction isolated from brain of mice with overexpressed (TgSOD2) or with reduced ($SOD2^{-/+}$) SOD2 as well as from those coming from the $p53^{-/-} \times$ TgSOD2 and $p53^{-/-} \times SOD^{-/+}$ mice. We observed an increase of ~25% in 3-NT levels in TgSOD2 compared with WT mice (Fig. 1C). Similary, an increase of PC in $SOD2^{-/+}$ mice was observed (Fig. 1A). The mice carrying the double mutation were characterized by a different behavior. Indeed, a significant ~40% reduction of PC (Fig. 1A) together with an increase of 3-NT levels (~30%; Fig. 1C) was observed in mitochondria from $p53^{-/-} \times SOD2^{-/+}$ mice compared with $SOD2^{-/+}$ mice. Furthermore, mitochondria from $p53^{-/-} \times$ TgSOD2 mice showed a reduction of ~30% in 3-NT levels compared with TgSOD2 (Fig. 1C).

Basal Oxidative and Nitrative Stress Levels Evaluated in Nuclei and Cytoplasm Isolated From Brain

To determine whether changes of basal oxidative and nitrative stress levels in mitochondria could also

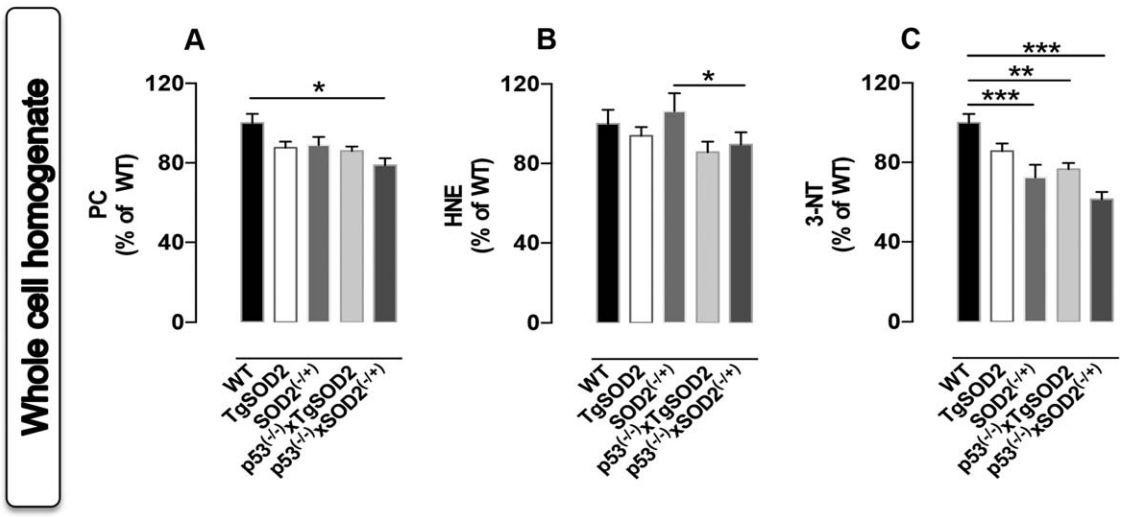

Fig. 3. In vivo oxidative and nitrative modifications observed in the whole homogenate obtained from the brains of WT, SOD2 transgenic (TgSOD2), and SOD2 heterozygous knockout ($SOD2^{-/+}$) mice and of mice carrying the double mutation ($p53^{-/-} \times$ TgSOD2, $p53^{-/-} \times SOD2^{-/+}$). PC (**A**), protein-bound HNE (**B**), and 3-NT (**C**) levels measured in the mitochondrial fraction. Densitometric values are percentage of the WT group, set as 100%. Data are mean ± SE of three replicates of each individual sample (n = 6) per group. $\star P < 0.05$, $\star\star P < 0.01$, and $\star\star\star P < 0.001$ vs. WT or the corresponding single-mutant mice (ANOVA).

promote changes in other subcellular compartements, PC, protein-bound HNE, and 3-NT levels were evaluated in both nuclear and cytosolic fractions. The nuclear fraction was characterized by a consistent increase of protein-bound HNE levels (~25%) in $p53^{-/-} \times SOD2^{-/+}$ mice compared with WT controls (Fig. 2B). p53 Deletion resulted in a significant increase of nuclear PC (~30%) and protein-bound HNE (~25%) in the nucleus of $p53^{-/-} \times SOD2^{-/+}$ mice compared with $SOD2^{-/+}$ mice (Fig. 2A,B). Conversely, deletion of p53 in TgSOD2 mice produced a significant reduction of 3-NT levels in the nucleus ($p53^{-/-} \times$ TgSOD2 vs. TgSOD2; Fig. 2C). In contrast to the changes observed in the nuclear and mitochondrial fractions, the cytosolic fraction was characterized by an overall reduction of the oxidative stress levels in the mice carrying the double mutation. In particular, a consistent reduction of protein-bound HNE levels was observed in both $p53^{-/-} \times$ TgSOD2 (~45%) and $p53^{-/-} \times SOD2^{-/+}$ (~30%) compared with both WT and single transgenic mice (Fig. 2E). Similarly, a reduction of ~15% was observed for PC in the same mice compared with WT mice (Fig. 2D). Furthermore, a decrease of ~10% in 3-NT levels was found in the cytosolic fraction isolated from $p53^{-/-} \times$ TgSOD2 compared with TgSOD2 mice (Fig. 2F).

Basal Oxidative and Nitrative Stress Levels Evaluated in Whole Homogenate From Brain

We then analyzed oxidative and nitrative stress levels in whole-brain homogenate to determine whether such levels reflect a sum of the events happening in the different cellular compartments. As shown in Figure 3A, a significant decrease of ~25% in PC levels was observed in $p53^{-/-} \times SOD2^{-/+}$ compared with WT mice. No significant changes were observed for HNE levels among all groups (Fig. 3B). A reduction of 3-NT levels occurred in $SOD2^{-/+}$ (~30%) as well as in $p53^{-/-} \times$ TgSOD2 (~25%) and in $p53^{-/-} \times SOD2^{-/+}$ (~40%) compared with WT mice (Fig. 3C). A reduction trend for both protein-bound HNE and 3-NT levels in the brain of $p53^{-/-} \times$ TgSOD2 and $p53^{-/-} \times SOD2^{-/+}$ compared with their matched single transgenic TgSOD2 and $SOD2^{-/+}$ mice was observed, although statistical significance was not achieved (Fig. 3B,C).

Proteins Involved in Cell Stress Response: the HO-1/BVR-A System and Thioredoxin-1

From the results obtained with regard to oxidative/nitrative stress levels in the subcellular compartments as well as in the whole homogenate, we sought to understand whether the observed changes could be associated with alterations of the levels of well-known proteins involved in cell stress response, such as the HO-1/BVR-A system and thioredoxin-1. Both HO-1 and thioredoxin-1 are membrane-bound proteins, whereas BVR-A is cytosolic. As shown in Figure 4A, HO-1 protein levels were significantly reduced in $SOD2^{-/+}$ mice by ~25% compared with WT mice. However, deletion of p53 in $SOD2^{-/+}$ mice promoted an upregulation of HO-1 protein ($p53^{-/-} \times SOD2^{-/+}$ vs. $SOD2^{-/+}$) to levels comparable to those observed in WT mice (Fig. 4A). In addition, the increase of HO-1 protein levels in $p53^{-/-} \times SOD2^{-/+}$ mice was negatively associated with PC levels in mitochondrial fraction (Pearson r = –0.58; Table II).

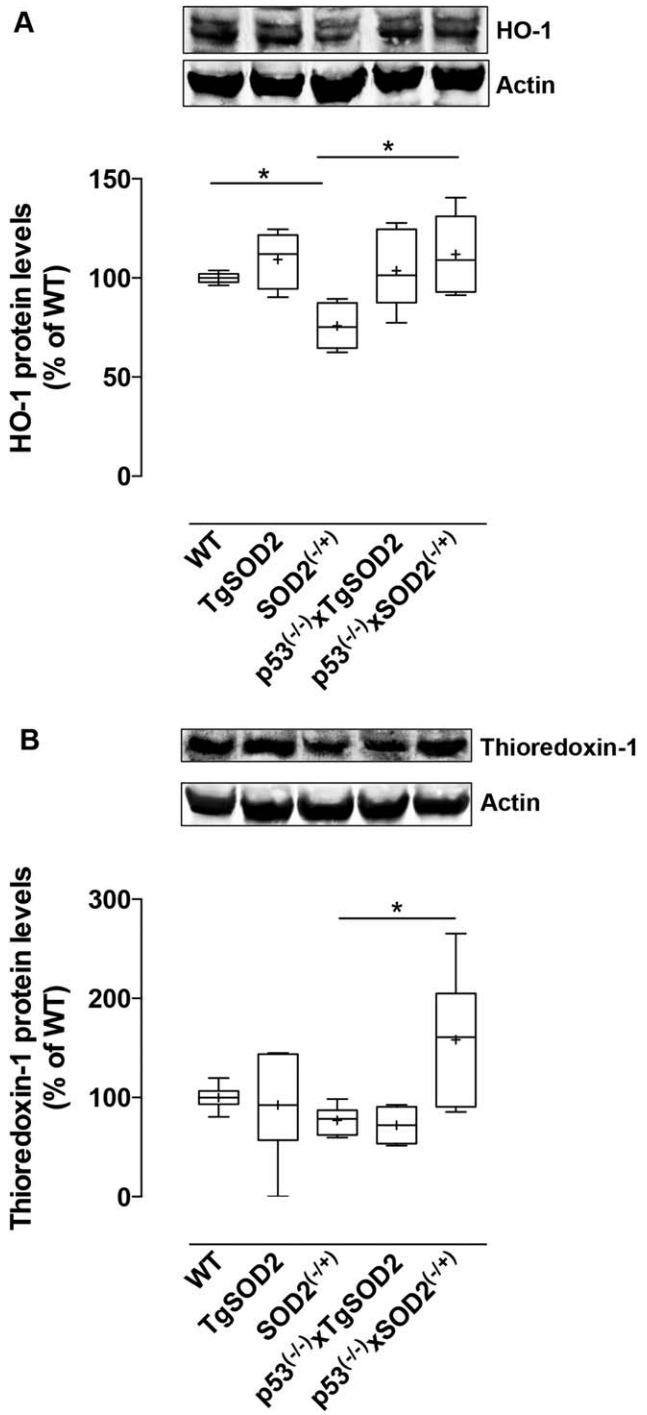

Fig. 4. HO-1 (**A**) and thioredoxin-1 (**B**) protein levels measured in the membrane fraction isolated from the brains of WT, SOD2 transgenic (TgSOD2), and SOD2 heterozygous knockout ($SOD2^{-/+}$) mice and of mice carrying the double mutation ($p53^{-/-} \times$ TgSOD2, $p53^{-/-} \times SOD2^{-/+}$), as described in Materials and Methods. Representative gels are shown. Protein levels were normalized to the loading control, β-actin. Densitometric values are percentage of the WT group, set as 100%. Data are mean ± SE of n = 6 individual samples per group. $\star P < 0.05$ vs. WT or the corresponding single-mutant mice (ANOVA).

Similarly to HO-1, thioredoxin-1 protein levels were almost doubled in $p53^{-/-} \times SOD2^{-/+}$ compared with $SOD2^{-/+}$ mice (Fig. 4B), and this effect was significantly and negatively associated with PC levels in whole-brain homogenate (Pearson r = –0.65; Table II). A decrease of ~20% was also observed in SOD-/+ compared with WT mice, although this value did not reach statistical significance (Fig. 4B).

The analysis of BVR-A revealed a trend that matched the elevation of its partner, HO-1. Indeed, the major result was the elevation of BVR-A protein levels observed in the cytosolic fraction of $p53^{-/-} \times SOD2^{-/+}$ mice compared with both WT (~35%) and $SOD2^{-/+}$ (~45%) mice (Fig. 5A). Increased cytosolic BVR-A in $p53^{-/-} \times SOD2^{-/+}$ mice was significantly and negatively associated with 3-NT (Pearson r = –0.74) and PC (Pearson r = –0.62) levels evaluated in whole-brain homogenate obtained from WT and $SOD2^{-/+}$ mice, respectively (Table II). These observations are in agreement with the well-known function of the HO-1/BVR-A system, whose final product, bilirubin, has been shown to possess significant antioxidant and antinitrative activities (Stocker et al., 1987a,b; Dore et al., 1999; Takahashi et al., 2000; Mancuso et al., 2003; Barone et al., 2009).

Because BVR-A is able to translocate into the nucleus, where it regulates the expression of stress-responsive genes such as HO-1 (Tudor et al., 2008) and iNOS (Gibbs et al., 2012; Di Domenico et al., 2013), we also evaluated nuclear BVR-A levels. Our results show a significant increase of ~80% in BVR-A nuclear levels in $p53^{-/-} \times SOD2^{-/+}$ compared with both WT and $SOD2^{-/+}$ mice (Fig. 4B). The increased translocation of BVR-A observed in the nucleus of $p53^{-/-} \times SOD2^{-/+}$ mice was positively associated with the elevation of HO-1 protein levels (Pearson r = 0.82; Table II). Consistent with this result and with the antioxidant role of BVR-A, several significant and negative correlations between BVR-A levels and oxidative stress markers were found (Table II), suggesting that, among the proteins analyzed, BVR-A could have a main role in cell stress response because of its pleiotropic functions (Kapitulnik and Maines, 2009; Barone et al., 2014).

Because both HO-1 and thioredoxin-1 levels are under control of the Nrf-2 nuclear transcriptional factor, we evaluated Nrf-2 levels both in the cytosolic and in the nuclear fractions. A significant 25% reduction of Nrf-2 levels in $SOD2^{-/+}$ compared with WT mice was observed (Fig. 6A). Evaluation of nuclear Nrf-2 levels revealed a consistent reduction in all the transgenic animals compared with WT animals (Fig. 6B).

DISCUSSION

This study provides new data on changes of basal oxidative and nitrative stress levels as a consequence of reduced or increased SOD2 levels in mouse brain. Specifically, we show that 1) basal oxidative and nitrative stress levels are differentially modulated depending on the cellular compartment examined; 2) these differences could be

TABLE II. Significant Correlations Found Between the Markers of Oxidative/Nitrosative Stress and the Proteins Involved in Cell Stress Response

	Variables			
Groups	X	Y	R	Pearson
WT vs. $p53^{-/-} \times SOD2^{-/+}$	BVR-A cytosolic	3-NT full homogenate	−0.74	0.03
$SOD2^{-/+}$ vs. $p53^{-/-} \times SOD2^{-/+}$	BVR-A cytosolic	PC full homogenate	−0.62	0.02
WT vs. $p53^{-/-} \times SOD2^{-/+}$	BVR-A nuclear	HNE cytosolic	−0.61	0.05
		3-NT cytosolic	−0.70	0.02
		PC full homogenate	−0.68	0.03
$SOD2^{-/+}$ vs. $p53^{-/-} \times SOD2^{-/+}$	BVR-A nuclear	3-NT nuclear	−0.75	0.01
		HNE cytosolic	−0.70	0.02
$SOD2^{-/+}$ vs. $p53^{-/-} \times SOD2^{-/+}$	HO-1	PC mitochondrial	−0.58	0.06
$SOD2^{-/+}$ vs. $p53^{-/-} \times SOD2^{-/+}$	Thioredoxin-1	PC full homogenate	−0.65	0.04
$SOD2^{-/+}$ vs. $p53^{-/-} \times SOD2^{-/+}$	BVR-A nuclear	HO-1	0.82	0.004

dependent, at least in part, on a different modulation of systems involved in the cell stress response; and 3) p53 affects the redox status of the cells, depending on SOD2 levels.

Mitochondria are both oxygen sensors and oxygen consumers, being the place deputed to the respiration processes and thus the dysregulation of SOD2 activity, which could alter oxygen concentration, resulting in adaptive responses aimed to protect the whole cell from further damage (Chandel et al., 2000).

Our data appear to be in line with this concept, given that we found increased protein oxidation (Fig. 1A) and increased protein nitration (Fig. 1C) only in mitochondria isolated from $SOD^{-/+}$ and TgSOD2 mice, respectively. Indeed, these changes do not affect the other cellular compartments (i.e., nucleus and cytoplasm; Fig. 2). Rather, an overall reduction of 3-NT levels in the whole-brain homogenate was observed (Fig. 3C). The increase of mitochondrial PC in $SOD2^{-/+}$ mice is consistent with the proposed antioxidant role of SOD2 (Williams et al., 1998; Miao and St. Clair, 2009), whereas the increase of mitochondrial 3-NT levels in TgSOD2 mice could result from the well-known ability of SOD2-derived H_2O_2 to induce NOS and thus NO production (Shimizu et al., 2003; Ha et al., 2005; Chucharoen et al., 2007). Although the observation that no changes with regard to PC or protein-bound HNE levels were found in the whole-brain homogenate obtained from both $SOD2^{-/+}$ and TgSOD2 mice is in agreement with a previous work (Ibrahim et al., 2013), it remains to be understood why a reduction of 3-NT levels has been observed.

One conceivable explanation comes from the differential effects produced by neurons and astrocytes. Our results were obtained in cellular fractions isolated from the whole-brain homogenate, and, because astrocytes outnumber neurons in the brain (Nedergaard et al., 2003), it is conceivable that this difference in terms of quantity would affect the final outcomes, probably resulting from compensation or adaptive mechanisms. For example, it has previously been reported that the relative abundance of newly born astrocytes is five- to ninefold higher in $SOD2^{-/+}$ mice compared with WT controls (Fishman et al., 2009). Unfortunately, we do not have any data on that from the other mouse models considered in this study, so we can only speculate about different possibilities. Because astrocytes are responsible for vital functions in the central nervous system, including glutamate, ion and water homeostasis, defense against oxidative stress, energy storage in the form of glycogen; scar formation, tissue repair, modulation of synaptic activity via the release of gliotransmitters, and synapse formation and remodeling (Belanger et al., 2011), a variation in astrocyte number could greatly impact the observed results. However, the other side of the coin must be considered. Two main aspects, very different between neurons and astrocytes, could be helpful in explaining the observed variations on basal oxidative/nitrative stress levels: the energetic metabolism and the antioxidant content. Indeed, although neurons rely on oxidative metabolism to meet their high energy requirements, astrocytes do not because their profile is highly glycolytic (Belanger et al., 2011). Paradoxically, neurons display limited defense mechanisms against oxidative stress compared with astrocytes. Indeed, astrocytes are characterized by higher levels of various antioxidant molecules and ROS-detoxifying enzymes such as glutathione (GSH), HO-1, GPx, GSH-S-transferase, catalase, and thioredoxin-1 (Belanger et al., 2011). In this scenario, changes in basal SOD2 levels/activity, which seem to affect mainly mitochondria oxidative/nitrative stress levels (Fig. 1), could be more deleterious for neurons. Indeed, because of their activities, neurons sustain a high rate of oxidative metabolism, so they appear to be very sensitive to mitochondrial damage (Belanger et al., 2011). On the other hand, this increase observed in mitochondrial oxidative/nitrative stress levels can be blunted by astrocytes, which, being more resistant than neurons, could provide the antioxidant defense to avoid further damage (Belanger et al., 2011). This hypothesis appears to be in line with our results in the whole-brain homogenate when any increase of PC, HNE, or 3-NT has been observed (Fig. 3).

Although this study provides compelling evidence for the role of oxidative/nitrative stress in brain

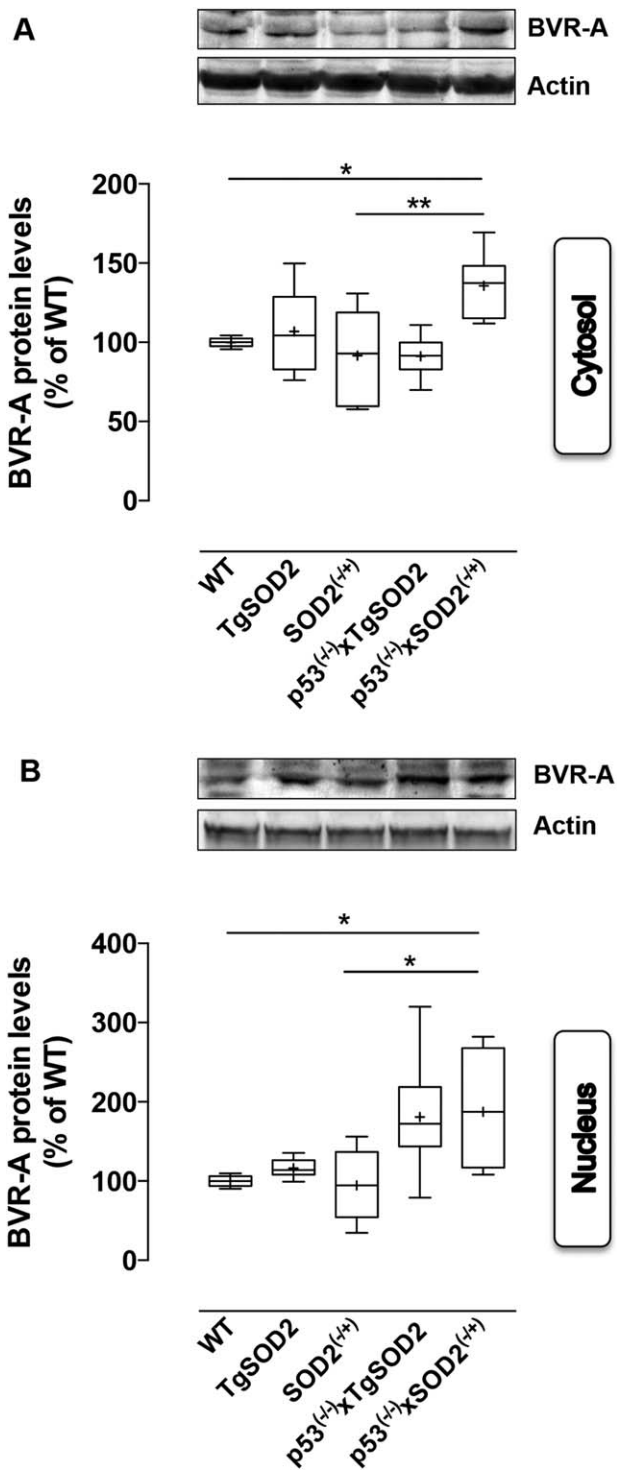

Fig. 5. Cytosolic (**A**) and nuclear (**B**) BVR-A protein levels measured in the brains of WT, SOD2 transgenic (TgSOD2), and SOD2 heterozygous knockout ($SOD2^{-/+}$) mice and of mice carrying the double mutation ($p53^{-/-} \times$ TgSOD2, $p53^{-/-} \times SOD2^{-/+}$), as described in Materials and Methods. Representative gels are shown. Protein levels were normalized to the loading control, β-actin. Densitometric values are percentage of the WT group, set as 100%. Data are mean ± SE of n = 6 individual samples per group. $^{\star}P < 0.05$, $^{\star\star}P < 0.01$ vs. WT or the corresponding single-mutant mice (ANOVA).

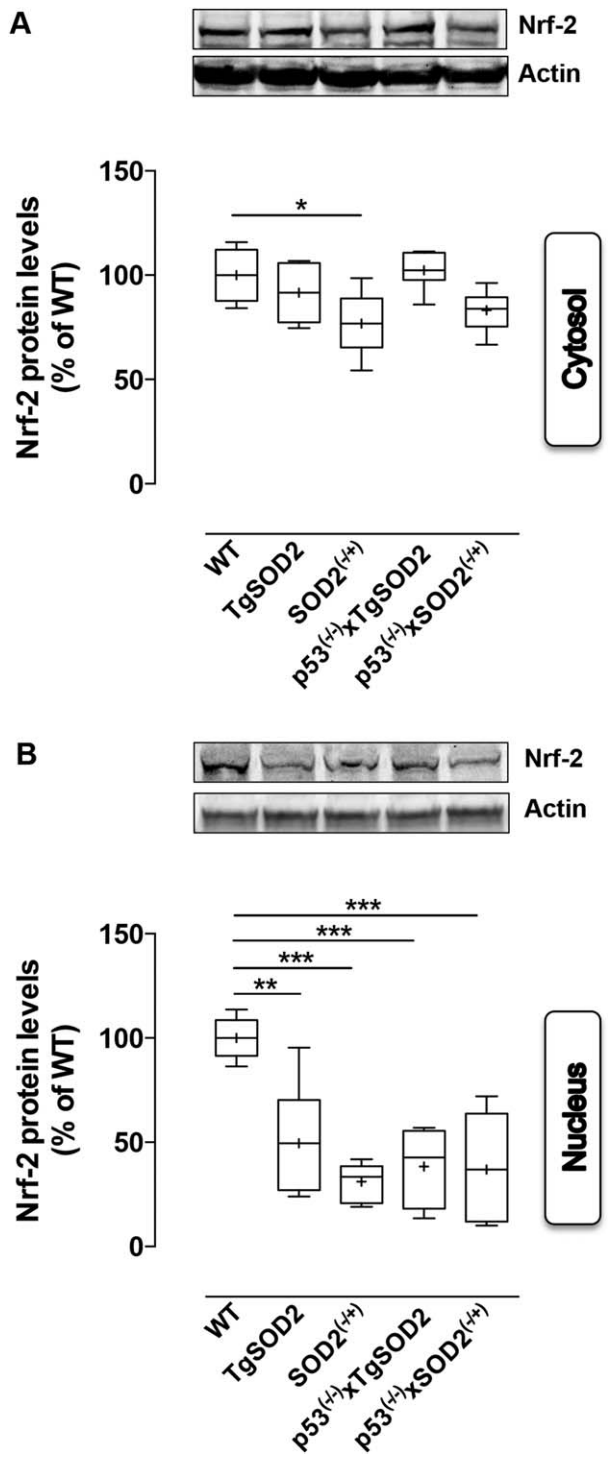

Fig. 6. Cytosolic (**A**) and nuclear (**B**) Nrf-2 protein levels measured in the brains of WT, SOD2 transgenic (TgSOD2), and SOD2 heterozygous knockout ($SOD2^{-/+}$) mice and of mice carrying the double mutation ($p53^{-/-} \times$ TgSOD2, $p53^{-/-} \times SOD2^{-/+}$), as described in Materials and Methods. Representative gels are shown. Protein levels were normalized to the loading control, β-actin. Densitometric values are percentage of the WT group, set as 100%. Data are mean ± SE of n = 6 individual samples per group. $^{\star}P < 0.05$, $^{\star\star}P < 0.01$, and $^{\star\star\star}P < 0.001$ vs. WT or the corresponding single-mutant mice (ANOVA).

physiopathology, we cannot exclude, as a plausible consequence, a role for nitrosative stress. Mild oxidative stress, which can derive from mitochondrial dysfunction, is able to induce different cellular signaling pathways and molecular mechanisms that mediate hormetic adaptive response (V. Calabrese et al., 2010, 2012; E.J. Calabrese et al., 2012). This response typically involves the synthesis of various stress-resistance proteins as the products of vitagenes, a group of genes strictly involved in preserving cellular homeostasis during stressful conditions, including both thioredoxin-1 and the HO-1/BVR-A system (V. Calabrese et al., 2010, 2012; E.J. Calabrese et al., 2012; Edrey et al., 2014). Thioredoxin-1 is involved in a variety of redox-dependent pathways, such as supplying reducing equivalents for ribonucleotide reductase and peptide methionine sulfoxide reductase, the latter being involved in antioxidant defense (Arner and Holmgren, 2000; Hirota et al., 2002). Similarly, the HO-1/BVR-A system catalyzes the transformation of the pro-oxidant heme into bilirubin (BR; Barone et al., 2014), which has been shown to possess strong antioxidant and antinitrative properties (Stocker et al., 1987a,b; Dore et al., 1999; Takahashi et al., 2000; Barone et al., 2009; Mancuso et al., 2012;). In addition to this canonical role, this system has several pleiotropic functions that are of interest in the regulation of the cell stress response (for review see Kapitulnik and Maines, 2009; Gozzelino et al., 2010).

Despite the observed changes in mitochondrial oxidative and nitrative stress marker levels in $SOD2^{-/+}$ and TgSOD2 mouse brain (Fig. 1A,C), the analysis of thioredoxin-1 and the HO-1/BVR-A system did not reveal any particular difference compared with WT, with the exception of a significant reduction of HO-1 in $SOD2^{-/+}$ mice (Fig. 4A). These lines of evidence seem to be supported by the reduced translocation of Nrf-2 protein to the nucleus (Fig. 6B). Indeed, following increased oxidative/nitrative stress levels, Nrf-2 is one of the main transcription factors that translocates into the nucleus, where it recognizes the antioxidant response element sequence on the promoter of the genes encoding for both HO-1 and thioredoxin-1, thus promoting their expression (Kim et al., 2001; Sun et al., 2002; Calabrese et al., 2009). Data for Nrf-2 seem to be in agreement with what we observed in the whole-brain homogenate (Fig. 3), suggesting that, under basal conditions, the reduction or the increase of SOD2 protein levels produces changes in mitochondria, which finally do not spread to the rest of the cell in terms of oxidative and nitrative stress. Because we are looking at a single age (6 months) without stimulation with toxic stimuli and because the evaluation of the oxidative/nitrative stress markers is an index of the oxidative damage accumulated over the time, it is conceivable that mitochondrial damage occurs quite early in the life of these mice as a consequence of SOD2 dysregulation and that this event is followed by the activation of the antioxidant response to avoid further damage. Thus, the absence of variations with regard to thioredoxin-1 and the HO-1/BVR-A system that are observed at 6 months of age could be the result of previous changes. These findings are also in line with the hypothesized protective role suggested for astrocytes, which could provide neurons with antioxidants (i.e., BR or GSH) as cited above (Belanger et al., 2011).

To characterize further the mechanisms underlying the cell stress response in $SOD2^{-/+}$ and TgSOD2 mouse brain, we focused on the role of p53 because of the well-known interconnectivity between SOD2 and p53 (for review see Holley et al., 2010; Pani and Galeotti, 2011). Indeed, p53 inhibits SOD2 superoxide scavenging activity (Zhao et al., 2005) and regulates SOD2 protein levels in a dual way (at a low concentration p53 increases SOD2 protein levels, whereas at a high concentration p53 decreases SOD2 expression; Holley et al., 2010). Furthermore, we demonstrate that a lack of p53 significantly reduces brain basal protein oxidation and lipid peroxidation through an increase of SOD2, thioredoxin-1, and the HO-1/BVR-A system (Barone et al., 2012; Fiorini et al., 2012).

Here we provide new data on the effects produced by the reduction or the overexpression of SOD2 in the absence of p53 with regard to the oxidative damage produced in the brain, thus extending the knowledge about this signaling network. Our results are in line with a hypothesized pro-oxidant role for p53 in the brain in that p53 directly represses antioxidant genes to enhance ROS production (Chatoo et al., 2011). Indeed, deletion of the p53 gene in both $SOD2^{-/+}$ and TgSOD2 mice is associated with decreased oxidative/nitrative stress levels in both cytosolic and whole-brain homogenate. These data suggest that changes occurring at the mitochondrial level are probably more dependent on SOD2, whereas p53 could modulate other pathways involved in the cell stress response, given that increases in the thioredoxin-1 (Fig. 4B), HO-1 (Fig. 4A), and BVR-A (Fig. 5) protein levels were observed. The significant negative correlation found between thioredoxin-1, HO-1, or BVR-A and oxidative stress makers in the different cellular compartments (Table II) further supports this hypothesis.

It appears that, after an initial damage that affects not only mitochondria but also the nucleus, the cell activates other antioxidant systems with the aim of preserving its integrity. These effects seems to be dependent, at least in part, on p53 (Barone et al., 2012) and are probably further promoted in the absence of the antioxidant SOD2, given that the overexpression of SOD2 emerges as being enough to promote comparable outcomes in terms of total oxidative stress levels (Fig. 3).

CONCLUSIONS

This study sheds light on the intricate mechanism(s) contributing to the maintenance of the redox status in the brain. The interconnectivity between p53 and SOD2 and the essential role of this latter protein as "guardian of the powerhouse" (Holley et al., 2011) for preventing cellular damage are further supported by our findings that, in the absence of p53 and reduced SOD2 levels, the cell must

activate other antioxidant systems, including the thioredoxin-1 and HO-1/BVR-A systems.

CONFLICT OF INTEREST STATEMENT

All authors state that they have no conflicts of interest associated with the research presented in this article.

ROLE OF AUTHORS

All authors had full access to all the data in this study and take responsibility for the integrity of the data and the accuracy of the data analysis. Study concept and design: EB, DAB. Acquisition of data: EB, GC, FDD. Analysis and interpretation of data: EB, GC, TN. Drafting of the manuscript: EB, DS, DAB. Critical revision of the article for important intellectual content: MP, DS, DAB. Statistical analysis: EB, MP, CW. Obtained funding: DS, DAB. Study supervision: DAB.

REFERENCES

Arner ES, Holmgren A. 2000. Physiological functions of thioredoxin and thioredoxin reductase. Eur J Biochem 267:6102–6109.

Barone E, Trombino S, Cassano R, Sgambato A, De Paola B, Di Stasio E, Picci N, Preziosi P, Mancuso C. 2009. Characterization of the S-denitrosylating activity of bilirubin. J Cell Mol Med 13:2365–2375.

Barone E, Cenini G, Sultana R, Di Domenico F, Fiorini A, Perluigi M, Noel T, Wang C, Mancuso C, St. Clair DK, Butterfield DA. 2012. Lack of p53 decreases basal oxidative stress levels in the brain through upregulation of thioredoxin-1, biliverdin reductase-A, manganese superoxide dismutase, and nuclear factor kappa-B. Antioxid Redox Signal 16:1407–1420.

Barone E, Di Domenico F, Mancuso C, Butterfield DA. 2014. The Janus face of the heme oxygenase/biliverdin reductase system in Alzheimer disease: it's time for reconciliation. Neurobiol Dis 62:144–159.

Belanger M, Allaman I, Magistretti PJ. 2011. Brain energy metabolism: focus on astrocyte–neuron metabolic cooperation. Cell Metab 14:724–738.

Calabrese EJ, Iavicoli I, Calabrese V. 2012. Hormesis: why it is important to biogerontologists. Biogerontology 13:215–235.

Calabrese V, Mancuso C, Calvani M, Rizzarelli E, Butterfield DA, Stella AM. 2007. Nitric oxide in the central nervous system: neuroprotection versus neurotoxicity. Nat Rev Neurosci 8:766–775.

Calabrese V, Cornelius C, Mancuso C, Barone E, Calafato S, Bates T, Rizzarelli E, Kostova AT. 2009. Vitagenes, dietary antioxidants, and neuroprotection in neurodegenerative diseases. Front Biosci 14:376–397.

Calabrese V, Cornelius C, Dinkova-Kostova AT, Calabrese EJ, Mattson MP. 2010. Cellular stress responses, the hormesis paradigm, and vitagenes: novel targets for therapeutic intervention in neurodegenerative disorders. Antioxid Redox Signal 13:1763–1811.

Calabrese V, Cornelius C, Dinkova-Kostova AT, Iavicoli I, Di Paola R, Koverech A, Cuzzocrea S, Rizzarelli E, Calabrese EJ. 2012. Cellular stress responses, hormetic phytochemicals, and vitagenes in aging and longevity. Biochim Biophys Acta 1822:753–783.

Chandel NS, Vander Heiden MG, Thompson CB, Schumacker PT. 2000. Redox regulation of p53 during hypoxia. Oncogene 19:3840–3848.

Chatoo W, Abdouh M, Bernier G. 2011. p53 Pro-oxidant activity in the central nervous system: implication in aging and neurodegenerative diseases. Antioxid Redox Signal 15:1729–1737.

Chucharoen P, Chetsawang B, Putthaprasart C, Srikiatkhachorn A, Govitrapong P. 2007. The presence of melatonin receptors and inhibitory effect of melatonin on hydrogen peroxide-induced endothelial nitric oxide synthase expression in bovine cerebral blood vessels. J Pineal Res 43:35–41.

Cobb CA, Cole MP. 2015. Oxidative and nitrative stress in neurodegeneration. Neurobiol Dis (E-pub ahead of print).

Di Domenico F, Perluigi M, Barone E. 2013. Biliverdin reductase-A correlates with inducible nitric oxide synthasein in atorvastatin treated aged canine brain. Neural Regen Res 8:1925–1937.

Dore S, Takahashi M, Ferris CD, Zakhary R, Hester LD, Guastella D, Snyder SH. 1999. Bilirubin, formed by activation of heme oxygenase-2, protects neurons against oxidative stress injury. Proc Natl Acad Sci U S A 96:2445–2450.

Duttaroy A, Paul A, Kundu M, Belton A. 2003. A Sod2 null mutation confers severely reduced adult life span in *Drosophila*. Genetics 165:2295–2299.

Edrey YH, Oddo S, Cornelius C, Caccamo A, Calabrese V, Buffenstein R. 2014. Oxidative damage and amyloid-beta metabolism in brain regions of the longest-lived rodents. J Neurosci Res 92:195–205.

Fiorini A, Sultana R, Barone E, Cenini G, Perluigi M, Mancuso C, Cai J, Klein JB, St. Clair D, Butterfield DA. 2012. Lack of p53 affects the expression of several brain mitochondrial proteins: insights from proteomics into important pathways regulated by p53. PLoS One 7:e49846.

Fishman K, Baure J, Zou Y, Huang TT, Andres-Mach M, Rola R, Suarez T, Acharya M, Limoli CL, Lamborn KR, Fike JR. 2009. Radiation-induced reductions in neurogenesis are ameliorated in mice deficient in CuZnSOD or MnSOD. Free Radic Biol Med 47:1459–1467.

Flynn JM, Melov S. 2013. SOD2 in mitochondrial dysfunction and neurodegeneration. Free Radic Biol Med 62:4–12.

Gibbs PE, Miralem T, Lerner-Marmarosh N, Tudor C, Maines MD. 2012. Formation of ternary complex of human biliverdin reductase-protein kinase Cdelta-ERK2 protein is essential for ERK2-mediated activation of Elk1 protein, nuclear factor-kappaB, and inducible nitric-oxidase synthase (iNOS). J Biol Chem 287:1066–1079.

Gozzelino R, Jeney V, Soares MP. 2010. Mechanisms of cell protection by heme oxygenase-1. Annu Rev Pharmacol Toxicol 50:323–354.

Gregory EM, Fridovich I. 1973. Oxygen toxicity and the superoxide dismutase. J Bacteriol 114:1193–1197.

Ha MK, Chung KY, Bang D, Park YK, Lee KH. 2005. Proteomic analysis of the proteins expressed by hydrogen peroxide treated cultured human dermal microvascular endothelial cells. Proteomics 5:1507–1519.

Hancock JT, Desikan R, Neill SJ. 2001. Role of reactive oxygen species in cell signalling pathways. Biochem Soc Trans 29:345–350.

Hirota K, Nakamura H, Masutani H, Yodoi J. 2002. Thioredoxin superfamily and thioredoxin-inducing agents. Ann N Y Acad Sci 957:189–199.

Holley AK, Dhar SK, St. Clair DK. 2010. Manganese superoxide dismutase versus p53: the mitochondrial center. Ann N Y Acad Sci 1201:72–78.

Holley AK, Bakthavatchalu V, Velez-Roman JM, St. Clair DK. 2011. Manganese superoxide dismutase: guardian of the powerhouse. Int J Mol Sci 12:7114–7162.

Holmstrom KM, Finkel T. 2014. Cellular mechanisms and physiological consequences of redox-dependent signalling. Nat Rev Mol Cell Biol 15:411–421.

Ibrahim WH, Habib HM, Kamal H, St. Clair DK, Chow CK. 2013. Mitochondrial superoxide mediates labile iron level: evidence from Mn-SOD-transgenic mice and heterozygous knockout mice and isolated rat liver mitochondria. Free Radic Biol Med 65:143–149.

Jang YC, Van Remmen H. 2009. The mitochondrial theory of aging: insight from transgenic and knockout mouse models. Exp Gerontol 44:256–260.

Jang YC, Perez VI, Song W, Lustgarten MS, Salmon AB, Mele J, Qi W, Liu Y, Liang H, Chaudhuri A, Ikeno Y, Epstein CJ, Van Remmen H, Richardson A. 2009. Overexpression of Mn superoxide dismutase does not increase life span in mice. J Gerontol A Biol Sci Med Sci 64:1114–1125.

Kapitulnik J, Maines MD. 2009. Pleiotropic functions of biliverdin reductase: cellular signaling and generation of cytoprotective and cytotoxic bilirubin. Trends Pharmacol Sci 30:129–137.

Kim YC, Masutani H, Yamaguchi Y, Itoh K, Yamamoto M, Yodoi J. 2001. Hemin-induced activation of the thioredoxin gene by Nrf2. A differential regulation of the antioxidant responsive element by a switch of its binding factors. J Biol Chem 276:18399–18406.

Li Y, Huang TT, Carlson EJ, Melov S, Ursell PC, Olson JL, Noble LJ, Yoshimura MP, Berger C, Chan PH, Wallace DC, Epstein CJ. 1995. Dilated cardiomyopathy and neonatal lethality in mutant mice lacking manganese superoxide dismutase. Nat Genet 11:376–381.

Mancuso C, Bonsignore A, Di Stasio E, Mordente A, Motterlini R. 2003. Bilirubin and S-nitrosothiols interaction: evidence for a possible role of bilirubin as a scavenger of nitric oxide. Biochem Pharmacol 66: 2355–2363.

Mancuso C, Barone E, Guido P, Miceli F, Di Domenico F, Perluigi M, Santangelo R, Preziosi P. 2012. Inhibition of lipid peroxidation and protein oxidation by endogenous and exogenous antioxidants in rat brain microsomes in vitro. Neurosci Lett 518:101–105.

Miao L, St. Clair DK. 2009. Regulation of superoxide dismutase genes: implications in disease. Free Radic Biol Med 47:344–356.

Miriyala S, Holley AK, St. Clair DK. 2011. Mitochondrial superoxide dismutase: signals of distinction. Anticancer Agents Med Chem 11:181–190.

Nedergaard M, Ransom B, Goldman SA. 2003. New roles for astrocytes: redefining the functional architecture of the brain. Trends Neurosci 26: 523–530.

Pani G, Galeotti T. 2011. Role of MnSOD and p66shc in mitochondrial response to p53. Antioxid Redox Signal 15:1715–1727.

Perluigi M, Coccia R, Butterfield DA. 2012. 4-Hydroxy-2-nonenal, a reactive product of lipid peroxidation, and neurodegenerative diseases: a toxic combination illuminated by redox proteomics studies. Antioxid Redox Signal 17:1590–1609.

Poon HF, Calabrese V, Scapagnini G, Butterfield DA. 2004. Free radicals and brain aging. Clin Geriatr Med 20:329–359.

Shimizu S, Shiota K, Yamamoto S, Miyasaka Y, Ishii M, Watabe T, Nishida M, Mori Y, Yamamoto T, Kiuchi Y. 2003. Hydrogen peroxide stimulates tetrahydrobiopterin synthesis through the induction of GTP-cyclohydrolase I and increases nitric oxide synthase activity in vascular endothelial cells. Free Radic Biol Med 34:1343–1352.

Sims NR. 1990. Rapid isolation of metabolically active mitochondria from rat brain and subregions using Percoll density gradient centrifugation. J Neurochem 55:698–707.

Stocker R, Glazer AN, Ames BN. 1987a. Antioxidant activity of albumin-bound bilirubin. Proc Natl Acad Sci U S A 84:5918–5922.

Stocker R, Yamamoto Y, McDonagh AF, Glazer AN, Ames BN. 1987b. Bilirubin is an antioxidant of possible physiological importance. Science 235:1043–1046.

Sultana R, Butterfield DA. 2008. Slot-blot analysis of 3-nitrotyrosine-modified brain proteins. Methods Enzymol 440:309–316.

Sun J, Hoshino H, Takaku K, Nakajima O, Muto A, Suzuki H, Tashiro S, Takahashi S, Shibahara S, Alam J, Taketo MM, Yamamoto M, Igarashi K. 2002. Hemoprotein Bach1 regulates enhancer availability of heme oxygenase-1 gene. EMBO J 21:5216–5224.

Takahashi M, Dore S, Ferris CD, Tomita T, Sawa A, Wolosker H, Borchelt DR, Iwatsubo T, Kim SH, Thinakaran G, Sisodia SS, Snyder SH. 2000. Amyloid precursor proteins inhibit heme oxygenase activity and augment neurotoxicity in Alzheimer's disease. Neuron 28:461–473.

Tudor C, Lerner-Marmarosh N, Engelborghs Y, Gibbs PE, Maines MD. 2008. Biliverdin reductase is a transporter of haem into the nucleus and is essential for regulation of HO-1 gene expression by haematin. Biochem J 413:405–416.

Van Remmen H, Ikeno Y, Hamilton M, Pahlavani M, Wolf N, Thorpe SR, Alderson NL, Baynes JW, Epstein CJ, Huang TT, Nelson J, Strong R, Richardson A. 2003. Life-long reduction in MnSOD activity results in increased DNA damage and higher incidence of cancer but does not accelerate aging. Physiol Genomics 16:29–37.

Williams MD, Van Remmen H, Conrad CC, Huang TT, Epstein CJ, Richardson A. 1998. Increased oxidative damage is correlated to altered mitochondrial function in heterozygous manganese superoxide dismutase knockout mice. J Biol Chem 273:28510–28515.

Zhao Y, Chaiswing L, Velez JM, Batinic-Haberle I, Colburn NH, Oberley TD, St. Clair DK. 2005. p53 Translocation to mitochondria precedes its nuclear translocation and targets mitochondrial oxidative defense protein-manganese superoxide dismutase. Cancer Res 65:3745–3750.

Zorov DB, Juhaszova M, Sollott SJ. 2006. Mitochondrial ROS-induced ROS release: an update and review. Biochim Biophys Acta 1757:509–517.